NMR, Relaxometric, and Structural Studies of the Hydration and Exchange Dynamics of Cationic Lanthanide Complexes of Macrocyclic Tetraamide Ligands

Silvio Aime,*,† Alessandro Barge,† James I. Bruce,‡ Mauro Botta,† Judith A. K. Howard,‡ Janet M. Moloney,‡ David Parker,*,‡ Alvaro S. de Sousa,‡ and Mark Woods‡

Contribution from the Department of Chemistry, University of Durham, South Road, Durham DH1 3LE, U.K., and Dipartimento di Chimica I.F.M., Universita degli Studi di Torino, via P. Giuria 7, 10125 Torino, Italy

Received January 22, 1999. Revised Manuscript Received April 22, 1999

Abstract: The solution structure and dynamics of metal-bound water exchange have been investigated in a series of lanthanide complexes of primary, secondary, and tertiary tetraamide derivatives of 1,4,7,10-tetraazacyclododecane. In the gadolinium complexes at ambient pH, water exchange lifetimes (τ_m) determined by ^{17}O NMR were sufficiently long (19 μs for [Gd·**2**]$^{3+}$, 298 K, 17 μs for [Gd·**3**]$^{3+}$, and 8 μs for [Gd·**4**]$^{3+}$) to limit the measured relaxivity. Direct ^1H NMR observation of the bound water resonance is possible for the corresponding Eu complexes at low temperature in CD_3CN, and the rate of water proton exchange is about 50 times faster in the twisted square antiprismatic isomer (m) than in the isomeric square antiprismatic (M) complex. The ratio of these two isomers in solution is sensitive to the steric demand of the amide substituent, with m/M = 2 for [Eu·**4**]$^{3+}$, but 0.25 for [Eu·**2**]$^{3+}$. The slowness of coordinated water exchange has allowed the rate of prototropic exchange to be studied: in basic media deprotonation of the bound water molecule or of proximate ligand amide NH protons leads to relaxivity enhancements, whereas in acidic media, hydration around the strongly ion-paired complexes is perturbed, facilitating water exchange. The X-ray crystal structure of ligand **3** reveals a hydrogen-bonded structure with two pairs of ring N-substituents related in a trans arrangement, contrasting with the structure of diprotonated DOTA in which the ligand is predisposed to bind metal ions. In the dysprosium complex [Dy·**3**·OH_2]$(PF_6)_3$, the metal ion adopts a regular monocapped square antiprismatic coordination geometry, with a water Dy−O bond length of 2.427(3) Å, and a PF_6 counterion is strongly hydrogen-bonded to this bound water molecule.

Introduction

There is considerable interest in understanding the salient features that determine the effectiveness of the paramagnetic contrast agents that are used to aid diagnosis in magnetic resonance imaging.[1] Water-soluble and kinetically robust gadolinium complexes have been devised which enhance the image contrast by increasing the water proton relaxation rate in the fluids and tissues where they are distributed. The preeminence of Gd(III) complexes for this purpose is a consequence of the long electronic relaxation time (T_{1e}) and high paramagnetism of the Gd^{3+} ion. The mechanism of the relaxation enhancement involves efficient dipolar magnetic coupling between the proton nuclear spins and the unpaired electrons of the Gd ion. There are three ways in which such coupling is believed to occur: first via dissociative exchange of the coordinated water molecule to the bulk (inner-sphere term); next via closely diffusing water molecules (outer-sphere term); finally via prototropic exchange of labile protons either in the water molecules bound to the metal or in the ligand which is used to chelate the gadolinium ion.[2] The importance of this prototropic exchange mechanism has been difficult to assess until recently, because the rate of molecular water exchange at the metal center is usually faster than the rate of proton exchange. It has become clear that the rate of dissociative water exchange in $q = 1$ gadolinium complexes is slower than had been originally surmised. For example, with the lanthanide aqua ions, the water exchange rate is of the order of 2×10^8 s^{-1}.[3] However, for the anionic complex $[Gd(DTPA)]^{2-}$ (DTPA = diethylenetriamine pentaacetate) the rate of water exchange, k_{ex} ($1/\tau_m$ where τ_m is the water exchange lifetime), is 5×10^6 s^{-1}, while in the related neutral complex [Gd(DTPA-BMA)] (DTPA-BMA = 1,7-bis-[(*N*-methylcarbamoyl)methyl]-1,4,7-triazaheptane 1,4,7-triacetate) k_{ex} has a value of 1.25×10^6 s^{-1}.[4] Therefore, in seeking to assess properly the relative importance of prototropic exchange, systems are required wherein the water exchange rate is somewhat slower than these values. It is important to highlight the role played by the rate of water exchange, as in the absence of prototropic exchange, it determines the efficiency of the transfer of the paramagnetic effect to bulk water and contributes directly to the modulation of the electron−nucleus dipolar interaction. The paramagnetic contribution to the measured water

* To whom correspondence should be addressed.
† Universita degli Studi di Torino.
‡ University of Durham.

(1) (a) Aime, S.; Botta, M.; Fasano, M.; Terreno, M. *Chem. Soc. Rev.* **1998**, *27*, 19. (b) Peters, J. A.; Huskens, J.; Raber, D. J. *Prog. NMR Spectrosc.* **1996**, *28*, 283. (c) Lauffer, R. B. *Chem. Rev.* **1987**, *87*, 901.

(2) (a) Meiboom, S. *J. Chem. Phys.* **1961**, *34*, 375. (b) Frey, U.; Merbach, A. E.; Powell, D. H. In *Dynamics of Solutions and Fluid Mixtures by NMR*; Delpuech, J.-J., Ed.; John Wiley & Sons Ltd.; Chichester, 1995; pp 263−307.

(3) Cossy, C.; Helm, A. E.; Merbach, A. E. *Inorg. Chem.* **1988**, *27*, 1973.

(4) (a) Gonzalez, G.; Powell, H. D.; Tissières, V.; Merbach, A. E. *J. Phys. Chem.* **1994**, *98*, 53. (b) Aime, S.; Botta, M.; Fasano, M.; Paoletti, S.; Anelli, P. L.; Uggeri, F.; Virtuani, M. *Inorg. Chem.* **1994**, *33*, 4707.

10.1021/ja990225d CCC: $18.00
Published on Web 06/05/1999

Chart 1

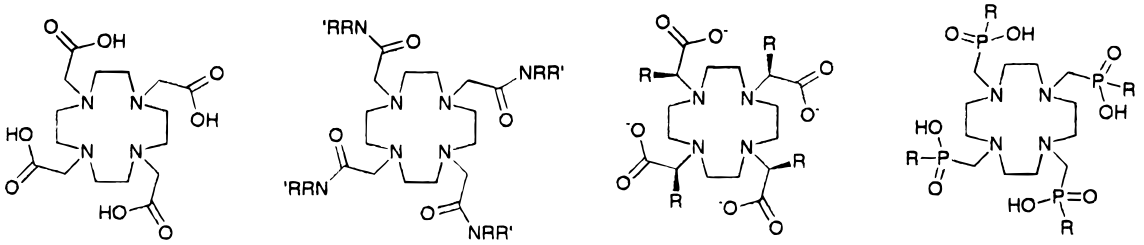

1 (dota)

2 R = R' = H (dotam)
3 R = H; R' = Me (dtma)
4 R = R' = Me (dotta)
5 R = H; R' = CHMePh

6 R = Me (dotma)
7 R = $CH_2CH_2CO_2H$

8 R = CH_3
9 R = CH_2Ph

proton relaxation rate (R_{1p}) is given by the sum of inner-sphere and outer-sphere terms (eq 1), and the inner-sphere contribution is given by eq 2

$$R_{1p} = R_{1p}^{is} + R_{1p}^{os} \quad (1)$$

$$R_{1p}^{is} = \frac{C_{tot}q}{55.6(T_{1m} + \tau_m)} \quad (2)$$

in Solomon−Bloembergen−Morgan theory,[1] where q is the number of bound water molecules, C_{tot} is the molar concentration of the paramagnetic complex, and T_{1m} is the longitudinal water proton relaxation time. If $\tau_m > T_{1m}$, then τ_m may determine the inner-sphere contribution to the observed relaxivity.

The observation that the water exchange rate in $q = 1$ complexes seemed to decrease as a function of the overall negative charge suggested that cationic complexes should be examined. Given that the lanthanide complexes of DOTA (tetraazacyclododecane tetraacetate), **1** (Chart 1), and its derivatives exhibit the highest kinetic and thermodynamic stability of all the commonly studied ligand systems,[5] we decided to study in detail the solution structure and dynamics of the tripositive lanthanide complexes of the tetraamides **2**, **3**, and **4** (Chart 1). The lanthanide complexes of the primary amide **2**[6a] and related tetraamides[6b,c] have been shown to be kinetically stable with respect to dissociation in the pH range 2 → 10. In addition, for complexes of Eu and Tb, the immediate neighbors of Gd in the lanthanide series, luminescence measurements have demonstrated unequivocally that one water molecule is bound in aqueous solution.[7] In principle, deprotonation of the bound water molecule or of the ligand amide NH protons in complexes of **3** and **4**[6b] affords a mechanism by which prototropic exchange may occur. Certain aspects of this work have been reported recently in preliminary communications.[8,9]

Results and Discussion

The primary amide ligand **2** (DOTAM),[6a,10] the *N*,*N*-dimethyl analogue **4** (DOTTA),[10,11] and the secondary amide **3** (DTMA)[10,12] were prepared using established procedures involving the alkylation of 1,4,7,10-tetraazacyclododecane with the appropriate α-haloamide derivative. The lanthanide complexes were prepared in anhydrous acetonitrile by reaction with the lanthanide trifluoromethanesulfonate salt, and were purified by repeated precipitation from CH_3CN/THF or by crystallization from an aqueous solution containing ammonium hexafluorophosphate. The ligand DTMA, **3**, also crystallized from aqueous basic solution, and its crystal structure has been compared to that of the ligand DOTA, which crystallized as the dihydrochloride salt from an aqueous solution (pH 3, dilute HCl). In the structure of **3**, there are two pairs of trans-related N-substituents, one in the plane of the 12-membered ring and one below. Strong intermolecular hydrogen bonds and contacts to water molecules determine the trans-disposition of the nitrogen pendant arms.

The first two protonations of such ligands occur on the 1,7-nitrogen atoms, so that in aqueous solution the ligand may be expected to take up a different conformation. This is highlighted in the structure of the N,N′-diprotonated form of DOTA, **1**, in which there are two orienting hydrogen bonds (N(1)H···O(4), 2.35 Å; N(3)H···O(6), 2.45 Å; see the Supporting Information for further details). The four nitrogen substituents are arranged on the same face of the 12-membered ring, and the protonated ligand structure closely resembles that found in its lanthanide complexes (Ln = Gd, Y, Lu)[13] in a manner which is reminiscent of the predisposed ligand and complex structures reported for the related tetrabenzylphosphinate derivative of tetraazacyclododecane.[14,15]

(5) (a) Spirlet, M. R.; Rebizant, J.; Loncin, M. F.; Desreux, J. F. *Inorg. Chem.* **1984**, *23*, 4278. (b) Harrison, A.; Walker, C. A.; Pereira, K. A.; Parker, D.; Royle, L.; Pulukkody, K.; Norman, T. J. *Magn. Reson. Imaging* **1993**, *11*, 761. (c) Parker, D. In *Comprehensive Supramolecular Chemistry*; Atwood, J. L., Davies J. E. D., MacNicol, D. D., Vögtle, F., Reinhoudt, D. N., Eds.; Pergamon: Oxford, 1996; Vol. 10, pp 487−536.

(6) (a) Amin, S.; Morrow, J. R.; Lake, C. H.; Churchill, M. R. *Angew. Chem., Int. Ed. Engl.* **1994**, **33**, 773. (b) Parker, D.; Williams, J. A. G. *J. Chem. Soc., Perkin Trans. 2* **1995**, 1305. (c) Dickins, R. S.; Howard, J. A. K.; Lehmann, C. W., Moloney. J. M.; Parker, D.; Peacock, R. D. *Angew. Chem., Int. Ed. Engl.* **1997**, 521.

(7) Dickins, R. S.; Parker, D.; de Sousa, A. S.; Williams, J. A. G. *Chem. Commun.* **1996**, 697. Beeby, A.; Clarkson, I. M.; Dickins, R. S.; Faulkner, S.; Parker, D.; Royle, L.; de Sousa, A. S.; Williams, J. A. G. *J. Chem. Soc., Perkin Trans. 2* **1999**, 493.

(8) Aime, S.; Barge, S.; Botta, S.; Parker, D.; de Sousa, A. S. *J. Am. Chem. Soc.* **1997**, *119*, 4767.

(9) Aime, S.; Barge, A.; Botta, M.; Parker, D.; de Sousa, A. S. *Angew. Chem., Int. Ed. Engl.* **1998**, *37*, 2673.

(10) DOTAM = 1,4,7,10-tetrakis[carbamoylmethyl]-1,4,7,10-tetraazacyclododecane, **2**; DTMA = 1,4,7,10-tetrakis[(*N*-methylcarbamoyl)methyl]-1,4,7,10-tetraazacyclododecane, **3**; DOTTA = 1,4,7,10-tetrakis[(*N*,*N*-dimethylcarbamoyl)methyl]-1,4,7,10-tetraazacyclododecane, **4**.

(11) Kataky, R.; Matthes, K. E.; Nicholson, P. E.; Parker, D.; Buschmann, H. J. *J. Chem. Soc., Perkin Trans. 2* **1990**, 1425.

(12) Alderighi, L.; Bianchi, A.; Calabi, L.; Dapporto, P.; Giorgi, C.; Losi, P.; Pateari, L.; Paoli, P.; Rossi, P.; Valtancoli, B.; Virtuani, M. *Eur. J. Inorg. Chem.* **1998**, 1581.

(13) (a) Dubost, J. P.; Leger, M.; Langlois, M.-H.; Meyer, D.; Schaefer, M. *C. R. Acad. Sci., Paris, Ser. 2* **1991**, *312*, 349. (b) Parker, D.; Pulukkody, K.; Smith, F. C.; Batsanov, A. S.; Howard, J. A. K. *J. Chem. Soc., Dalton Trans.* **1994**, 689. (c) Aime, S.; Barge, A.; Botta, M.; Fasano, M.; Ayala, J. D.; Bombieri, G. *Inorg. Chim. Acta* **1996**, *246*, 423.

(14) Aime, S.; Batsanov, A. S.; Botta, M.; Dickins, R. S.; Faulkner, S.; Foster, C. E.; Harrison, A.; Howard, J. A. K.; Moloney, J. M.; Norman, T. J.; Parker, D.; Royle, L.; Williams, J. A. G. *J. Chem. Soc., Dalton Trans.* **1997**, 3623.

(15) Aime, S.; Botta, M.; Parker, D.; Senanayake, K.; Williams, J. A. G.; Batsanov, A. S.; Howard, J. A. K. *Inorg. Chem.* **1994**, *33*, 4696.

Table 1. Selected Bond Distances (Å) and Angles (deg) for $[Dy\cdot\mathbf{3}](PF_6)_3$

Dy−O(2)	2.310(2)	N(3)−C(5)-C(6)−N(4)	−59.9(2)
Dy−O(4)	2.348(2)	N(1)−C(1)-C(2)−N(2)	−58.6(2)
Dy−O(1)	2.3495(14)	N(2)−C(3)-C(4)−N(3)	−58.1(2)
Dy−O(3)	2.4139(14)	N(1)−C(11)-C(12)−O(1)	33.5(3)
Dy−O(5)	2.427(2)	N(2)−C(21)-C(22)−O(1)	29.8(3)
Dy−N(3)	2.605(2)	O(2)−Dy-O(1)	84.68(5)
Dy−N(4)	2.640(2)	N(3)−Dy-N(4)	68.88(5)
Dy−N(1)	2.643(2)	O(4)−Dy-N(4)	66.95(5)
Dy−N(2)	2.654(2)	O(3)−Dy-O(5)	71.22(5)

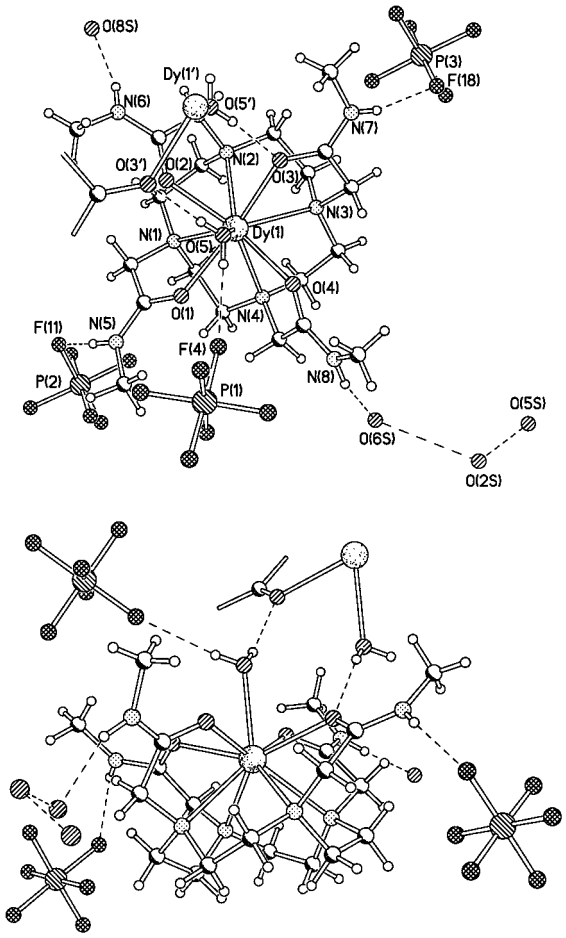

Figure 1. Structure of $[Dy\cdot\mathbf{3}\cdot OH_2](PF_6)_3$ in the crystal showing (a, top) a slightly offset view down the C_4 axis highlighting the monocapped square antiprismatic coordination about the nine-coordinate Dy ion, with N−C−C−N and N−C−C−O torsion angles averaging −58.7° and +30.6°, respectively, and (b, bottom) side elevation revealing the geometry about the Dy center and the position of the water molecules and the hexafluorophosphate anions; the disorder of the $P(1)F_6$ and $P(3)F_6$ anions is not shown. Water molecules, except O(5) and O(6S) are disordered: seven positions with 25% or 50% occupancies were located, of which only one compatible set of positions is shown.

Crystals of the dysprosium complex of **3** were grown from aqueous ammonium hexafluorophosphate solution, and the structure (Table 1 and Figure 1) revealed that the dysprosium was nine-coordinate, being bound to one water molecule (Dy−O = 2.427(2) Å) and the four ring nitrogen (mean Dy−N = 2.63 Å) and amide carbonyl oxygen atoms (mean Dy−O = 2.35 Å). The geometry about the dysprosium ion is a fairly regular monocapped square antiprism, with a twist angle (the relative rotational orientation of the N_4 and O_4 moieties) of 39° between the N_4 and O_4 planes. The structure closely resembles that reported recently for the enantiopure complex $[Dy\cdot\mathbf{5}(H_2O)](CF_3SO_3)_3$,[6c] and differs from the reported disordered structure of $[Eu\cdot\mathbf{1}(H_2O)](CF_3SO_3)_3$ in which there is a twisted square antiprismatic geometry about Eu,[17] with a 30° twist angle. The Dy-bound water molecule is strongly hydrogen-bonded to a PF_6 counterion, and in the lattice there is also a hydrogen bond to the carboxylate oxygen, O(3), of a second complex molecule. Thus, the cations (related via an inversion center) contact top-to-top and are linked in dimers by a pair of O(5)−H···O(3′) hydrogen bonds. Trans-related amide NH groups are also involved in hydrogen bonding: one pair form hydrogen bonds to proximate water molecules (O(8S) and O(6S)), while the other amide NH protons (N(7) and N(5)) are each bound to another PF_6 anion (Figure 1).

In the lanthanide complexes of DOTA, **1**, and its achiral analogues—such as **2**, **3**, and **4**—two structurally independent elements of chirality are present, defined by the pendant arm N−C−C−O and ring N−C−C−N torsion angles. The 12-membered ring may adopt two enantiomeric conformations, given as $\delta\delta\delta\delta$ or $\lambda\lambda\lambda\lambda$ (with respect to each five-ring chelate), and the pendant arms may be arranged in either a clockwise (Δ) or an anticlockwise (Λ) manner.[18] Interconversion between the four stereoisomers may occur via stepwise or synchronous arm rotation and ring inversion.[19] For $[Dy\cdot\mathbf{3}\cdot H_2O]^{3+}$, there are two enantiomeric complexes in the unit cell: the square antiprismatic complex shown in Figure 1 possesses N−C−C−N torsion angles averaging −58.7° and N−C−C−O angles averaging +30.6° consistent with a left-handed ring conformation ($\lambda\lambda\lambda\lambda$) and a right-handed ($\Delta$) helicity in the pendant arm layout.[18]

Kinetic Stability of Complexes. The lanthanide complexes of **2** have been shown to be moderately thermodynamically stable in aqueous solution, with ML formation constants on the order of 10^{13}.[12,16] As a result of their tripositive charge, they tend to resist protonation and so are kinetically stable with respect to acid-catalyzed dissociation. Indeed Morrow has reported that $[Eu\cdot\mathbf{2}]^{3+}$ has a half-life of 50 days at 60 °C and pH 2.[6a,17] A simple NMR procedure has been used in this work that allows an estimate of the kinetic stability of the lanthanide complexes under acidic conditions to be obtained. The analytically pure gadolinium complexes of **2**, **3**, and **4** were dissolved in 2.5 M nitric acid, and the decrease in the water proton relaxation time, T_1, was monitored at 293 K as a function of time. The decrease occurs following the release of the free aqua ion, which possesses a relaxivity value that is about 4−5 times higher than those of the complexes. Dissociation was observed to occur only very slowly under these conditions, over a period of several weeks. The data from such experiments allowed an estimate of the half-life for complex dissociation (with an estimated error of ±10%) and, in addition, from the value of T_1 extrapolated to infinite time, permitted an accurate value of the total gadolinium concentration to be calculated and hence the relaxivity of the starting solution. These concentration values were consistent with the total concentration of Gd measured independently by atomic absorption spectroscopy and by inductively coupled plasma mass spectrometry. The half-lives for dissociation (2.5 M HNO_3, 298 K) increased from 4.5 h for the anionic complex of DOTA $[Gd\cdot\mathbf{1}]^-$ to 68, 155, and 384 h

(16) Maumela, H., Hancock, R. D.; Carlton, C.; Reibenspies, J. H.; Wainwright, K. P. *J. Am. Chem. Soc.* **1995**, *117*, 6698.
(17) Amin, S., Voss, D. A.; Horrocks, W. de W.; Lake, C. H.; Churchill, M. R.; Morrow, J. R. *Inorg. Chem.* **1995**, *34*, 3294.
(18) Dickens, R. S.; Howard, J. A. K.; Maupin, C. L.; Moloney, J. M.; Parker, D.; Peacock, R. D.; Riehl, J. P.; Siligardi, G. *New. J. Chem.* **1998**, 891.
(19) Aime, S.; Botta, M.; Fasano, M.; Harques, M. P. M.; Geraldes, C. F. G. C.; Pubanz, D.; Merbach, A. E. *Inorg. Chem.* **1997**, *36*, 2059.

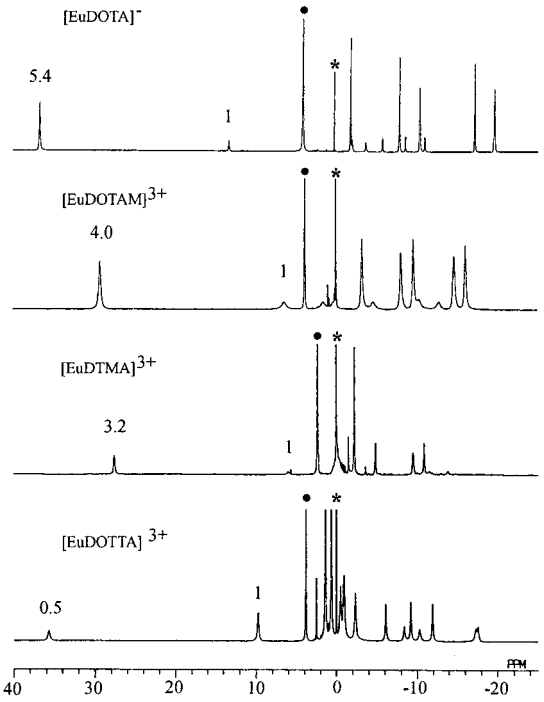

Figure 2. H NMR spectra (273 K, 400 MHz, pD 6) for [Eu·DOTA]$^-$ (top), [Eu·**2**]$^{3+}$, [Eu·**3**]$^{3+}$, and [Eu·**4**]$^{3+}$ showing the variation in the M/m isomer ratio as a function of the steric demand near the bound oxygens.

for the cationic complexes of DOTAM, **2**, DTMA, **3**, and DOTTA, **4**, respectively. The more sterically encumbered dimethylamide complex dissociated most slowly with a half-life under the cited conditions of 16 days! Consistent with this behavior, at room temperature and in the pH range 4−11, no traces of decomposition were evident from an examination of the shifted ^{1}H NMR spectra of the corresponding europium complexes in solution, over a period of several weeks. Between pH 1 and pH 4, the spectra remained unchanged over a period of at least 72 h. In particular the line width of the resonances was unchanged, as was observed with the corresponding Yb complexes, confirming the absence of any significant (<1%) dissociation.

Solution Speciation, Hydration, and Water Proton Exchange Dynamics. In aqueous solution, two diastereoisomeric species are present in complexes of DOTA with the central lanthanides, namely, the square antiprismatic complex (M) and the twisted square antiprismatic structure (m), with a different helicity around the metal center. When the two isomers are in slow exchange on the NMR time scale, two sets of six resonances are observed for the diastereotopic CH_2CO and ring NCH_2CH_2N protons. The ^{1}H NMR spectra of the three triamide complexes and of [Eu·DOTA]$^-$ are compared in Figure 2, under conditions where exchange between the isomers is slow on the NMR time scale (273 K, pD 5, 400 MHz), allowing the identification of each diastereoisomer. For [Eu·DOTA]$^-$, it has been established that the major isomer in solution adopts the square antiprismatic structure (M), characterized by a shift to high frequency of the closest of the ring axial protons ($\delta_{H_{ax}}$ = +36.5 ppm).[20] The minor isomer (m) generally exhibits less shifted proton resonances. The m/M isomer ratio increased from 0.19 for [Eu·DOTA]$^-$ to 0.25 for [Eu·**2**]$^{3+}$ and 0.31 for [Eu·**3**]$^{3+}$. In the case of [Eu·**4**]$^{3+}$, the twisted antiprismatic isomer was the major isomer observed in solution, with an m/M ratio of 2. This variation of isomer ratio accords with the general observation that increasing the steric demand at the bound metal ion favors the twisted square antiprismatic structure. Such behavior has been noted with the RRRR/SSSS α-alkylated analogues of DOTA, e.g., DOTMA, **6**, and the carboxyethyl analogue **7**[21,22] (Chart 1), where the m/M isomer ratio is also approximately 4:1 for their europium complexes. In the tetramethyl- and tetrabenzylphosphinate europium complexes, e.g., [Eu·**8**]$^-$ and [Eu·**9**]$^-$ (Chart 1), such is the steric demand around the four stereogenic phosphorus centers that only the twisted square antiprismatic structure (RRRR or SSSS at P) is evident in solution, and the bound lanthanide ion is eight-coordinate.[14,15] Of course, the isomer ratio m/M is a sensitive function of the size of the lanthanide ion and may also be perturbed by the concentration and nature of the counterion.[19,20] With the dysprosium complexes of **2** and **3**, the M isomer was strongly favored in solution (m/M < 0.12). For [Eu·**3**]$^{3+}$, the m/M isomer ratio was 0.31 in D_2O and decreased to 0.25 in CD_3OD, and in CD_3CN less than 7% of the twisted square antiprismatic isomer was evident at −40 °C. Clearly differential solvation of the two isomers is sufficient to perturb the relative concentrations of the two species.

The europium complexes of **1**−**4** have previously been shown to bind one water molecule in the pH range 2−9, by luminescence lifetime measurements in H_2O and D_2O.[7] In anhydrous acetonitrile, the rate constant for depopulation of the Eu excited state in a dried sample of [Eu·**3**]$^{3+}$ (298 K, 1 mM complex) was measured to be 0.74×10^3 s^{-1}, compared to a value of 1.82×10^3 s^{-1} in pure water. By measuring the variation of the rate of decay of the Eu luminescence at 618 nm ($\Delta J = 2$ transition) with added water concentration, the association constant for hydration of the Eu complex in CH_3CN was determined. Analysis of the resultant isotherm using a 1:1 binding model (i.e., ignoring the quenching effect of unbound water molecules, whose effect is only important at higher added water concentration) gave a value for K_a of 33(±4) M^{-1}. Therefore, at 298 K with a total water concentration of ca. 30 mM, 50% of the monohydrated and unhydrated complexes exist in solution.

This water molecule may be directly observed by ^{1}H NMR in dry CD_3CN: in the case of [Eu·**3**]$^{3+}$ (10 mM undried complex, 80 mM total water concentration—as determined by NMR integration of the coalesced water signal at 323 K versus the four-proton H_{axial} signal at ca. 30 ppm) the coordinated water resonated as an exchange-broadened singlet in the temperature range 0 to −40 °C, and at −40 °C it had a shift of +86.1 ppm. Water bound to the minor (m) isomer was also detected at +22.2 ppm. With the primary amide complex, [Eu·**2**]$^{3+}$, there was a higher proportion of the m isomer in solution at low temperature, and signals due to the bound water for each species were discerned at +84.1 (M) and +19.0 (m) ppm (232 K, CD_3CN). This assignment was confirmed by taking a sample of [Eu·**2**]$^{3+}$ that had undergone H/D exchange and running its ^{2}H NMR spectrum in CH_3CN at 232 K: the ^{2}H resonances for free and bound water were observed at the same chemical shift as in the ^{1}H NMR spectrum. In addition the ^{2}H NMR spectrum revealed resonances due to the diastereotopic $COND_2$ protons, which were evident at −5.6 and +1.4 ppm, respectively.

Variable-temperature ^{1}H NMR spectroscopy also provided details of the dynamics of water exchange in both the M and m isomers. For [Eu·**2**]$^{3+}$ (25 mM in CD_3CN, 400 mM total H_2O)

(20) Aime, S.; Botta, M.; Ermondi, G. *Inorg. Chem.* **1992**, *31*, 4291.

(21) Howard, J. A. K.; Kenwright, A. K.; Moloney, J. M.; Parker, D.; Port, M.; Navet, M.; Rousseau, O.; Woods, M. *Chem. Commun*. **1998**, 1381.

(22) Spirlet, M.; Rebizant, J.; Desreux, J. F.; Loncin, M.-F. *Inorg. Chem.* **1984**, *23*, 359.

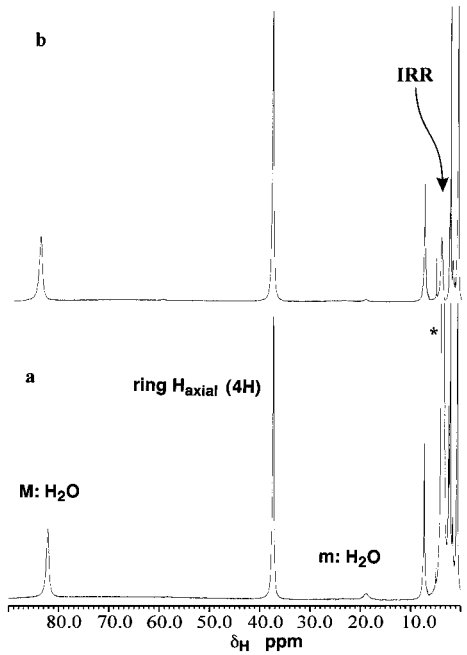

Figure 3. ^{1}H NMR spectrum of [Eu·**2**]$^{3+}$ at 235 K in CD_3CN showing (a) the bound water signals of the M and m isomers and (b) the effect of saturation of the free water signal.

the bound water proton resonance for the m isomer, at 400 MHz, broadened on raising the temperature above 230 K and disappeared at temperatures above 245 K—a temperature at which the rate of arm rotation and ring conversion is very slow on the NMR time scale (400 MHz). For the M isomer, the onset of exchange broadening was evident only at temperatures in excess of 273 K. Over the range 223−303 K, the free water signal (ca. +3.6 ppm) first broadened—with maximal line-broadening at 248 K—and then sharpened up, before broadening again at temperatures above 280 K. Selective irradiation of the signal due to free water at 232 K had almost no effect on the position and intensity of the resonance at +84.1 (M isomer, OH_2) but significantly reduced the intensity of the bound water signal due to the m isomer (Figure 3). Repeating this saturation transfer experiment at 283 K gave rise to saturation of the bound water signal in the M isomer. Such behavior is consistent with chemical exchange of free and bound water, which occurs at a different rate in each isomer. Line-shape analysis using the DNMR-SIM program, over the temperature range 239−306 K, allowed the rates of exchange at each temperature to be assessed. At 298 K in CD_3CN, the rate of water exchange was estimated to be 3.8(±1.5) × 10^5 s^{-1} for the minor isomer and 8.3(±2.0) × 10^3 s^{-1} for the square antiprismatic (M) isomer. The free energies of activation at 298 K were estimated to be $\Delta G^{\ddagger} = 41 \pm 2$ and 50.6 ± 2.5 kJ mol^{-1} for the m and M isomers, with a positive entropy of activation in each case.

The ratio of the two isomers for [Ln·**2**]$^{3+}$ in solution is sensitive to the nature of the lanthanide ion. In CD_3CN at 233 K, the m/M ratio was measured to be 8:1 for Ln = Pr, 4 for Nd, 1.5 for Sm, 0.4 for Eu, 0.06 for Tb, and 0.03 for Dy. Therefore, it is reasonable to estimate that there is no more than 10% of the m isomer for [Gd·**2**]$^{3+}$ at 233 K, and as the population of this isomer decreases with increasing *T*, there is likely to be less than 5% of the m isomer at temperatures above 273 K.

With [Eu·**3**]$^{3+}$, there was insufficient minor isomer present in solution at low temperatures to allow a reliable estimate of its exchange rate to be assessed. However, the rate of exchange of water in the M isomer was studied by saturation transfer and relaxation rate measurements in the range 260−280 K. Analysis of the ln *k* vs T^{-1} plot revealed that k_{298} = 6.4(±1.5) × 10^3 s^{-1}, similar to the value obtained with [Eu·**2**]$^{3+}$. The free energy of activation was estimated to be 51(±2.5) kJ mol^{-1}, with a large positive entropy of activation ($\Delta S^{\ddagger} = +148 \pm 35$ J mol^{-1} K^{-1}) consistent with a strongly dissociative exchange process in which there is a late transition state, wherein considerable loosening of the ordered hydration and ion-paired structure occurs.

Table 2. Summary of Relaxivity Data and Water and Proton Exchange Equilibria Obtained by Fitting the pH/Relaxivity Profiles to eqs 1, 2, and 8−11 (298 K, 20 MHz, triflate salts, 0.001 M)

	[Gd·DOTAM]$^{3+}$	[Gd·DTMA]$^{3+}$	[Gd·DOTTA]$^{3+}$
R_{1p} (mM^{-1} s^{-1})[a]	2.5	2.5	3.0
T_{1m} (μs)	5.5	5.5	5.5
τ_m (μs)	19	17	7.8
K_a (M)	1.1×10^{-7}	7.9×10^{-8}	8.5×10^{-8}
k_{aex} (s^{-1})	3.6×10^6	3.4×10^6	1.8×10^6
k_{bex} (s^{-1})	1.5×10^{12}	1.3×10^{11}	6.2×10^9
K_a' (M^2)	1.0×10^{-18}	8.1×10^{-20}	
w	2	2	
T_{1m}'' (μs)	18	18	
R_{os} (s^{-1})	1.8	1.8	1.8

[a] Relaxivity values are quoted at pH 6; under the same conditions, for [GdDOTA]$^-$, R_{1p} = 4.7 mM^{-1} s^{-1}.

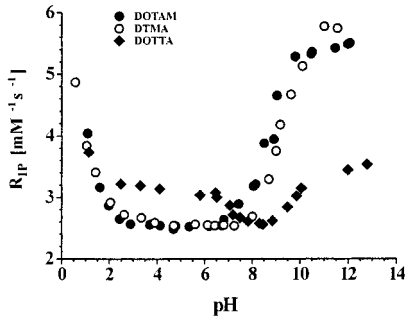

Figure 4. Relaxivity versus pH profiles for the triflate salts of [Gd·**2**]$^{3+}$, [Gd·**3**]$^{3+}$, and [Gd·**4**]$^{3+}$ (20 MHz, 298 K).

The important conclusion from these NMR studies is that dissociative water exchange at a lanthanide center occurs at a rate which is dependent upon the nature of the coordination geometry at the metal center. In the case of these DOTA-like complexes, exchange occurs around 50 times more rapidly, at 298 K, in the twisted square antiprismatic complex. Gadolinium complexes which prefer to adopt this geometry in solution will therefore possess an inner-sphere relaxivity which is less likely to be limited by the water exchange rate.

Relaxometric and ^{17}O NMR Investigations. The longitudinal relaxivity values for [Gd·DOTA]$^-$ and the three cationic tetraamide complexes were measured at 298 K (pH 6, 20 MHz; Table 2). The values found for the amide complexes are lower than that which is normally expected for a *q* = 1 complex.[1] The relaxivity of aqueous solutions of the triflate salts of the three amide complexes was markedly dependent upon solution pH (Figure 4). For [Gd·**2**]$(CF_3SO_3)_3$ and [Gd·**3**]$(CF_3SO_3)_3$, the relaxivity was constant over the pH range 3−8, but in either more acidic or more basic media there was a strong relaxation enhancement. The behavior of [Gd·**4**]$(CF_3SO_3)_3$ was distinctively different, and it showed a decrease of R_{1p} in the pH range 6−8 and then a much less pronounced increase in the basic pH region. The relaxivity of [Gd·DOTA]$^-$ is 4.7 mM s^{-1} over the pH range 2−12, and this same value was measured at pH 8.5 for [Gd·**2**]$^{3+}$ and 9.5 for [Gd·**3**]$^{3+}$.

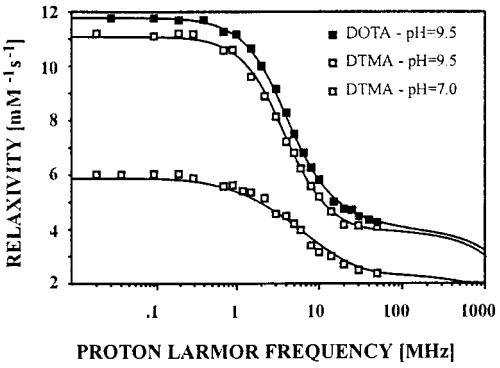

Figure 5. Comparison of the NMRD profiles for [Gd·DOTA]$^-$ and [Gd·**3**]$(CF_3SO_3)_3$ at pH 9.5 and 7.0 (298 K). The continuous line shows the fit to the experimental data.

The NMRD profile for [Gd·**3**]$(CF_3SO_3)_3$ was measured on the Koenig−Brown field cycling relaxometer at 298 K and pH 9.5 and is compared to that for [Gd·DOTA]$^-$ (Figure 5). The profile shows a single dispersion centered near 4 MHz and two plateaus in the regions of low and high magnetic fields. The high value of the relaxivity in the low-field region is indicative of a long value of the electronic relaxation time, as typically observed in the case of macrocyclic, highly symmetric Gd complexes. Indeed by adopting standard values for a, D, and r ($q = 1$) and fitting the profile using well-established procedures,[1] a long τ_{so} value is obtained (600 ps, as expected for a highly symmetric, relatively rigid Gd complex), along with a τ_r value of 80 ps (consistent with the size of the complex) and a τ_m value of about 30 ns. Such an approach is reasonable because it has been established that minor structural differences in "DOTA-like" complexes, while giving rise to significant changes in τ_s, do not significantly affect the NMRD profile, as it is dominated by τ_r. Thus, at this pH, the relaxivity of this tetraamide complex may be accounted for using structural and dynamic relaxation parameters that are very similar to those of the anionic complex [Gd·DOTA]$^-$. Such an analogy suggested that the marked pH dependence of the relaxivity was most likely to be related to the pH dependence of the proton exchange lifetime, for those labile protons which are close to the paramagnetic center. The experimental data for the relaxivity of [Gd·**3**]$^{3+}$ in the pH-independent region may now be fitted by keeping fixed all those parameters found at pH 9.5 (e.g., τ_{so} and τ_r) and allowing τ_m to vary. The result is that the data are fitted well for a value for τ_m of 19 μs, which is considerably longer than that found for any other Gd complex.[4] This long τ_m value substantially reduces the contribution of the inner-sphere component as $\tau_m \gg T_{1m}$ (slow exchange condition). The effect is further exemplified in the temperature dependence of the relaxivity, at a fixed field. Three distinct temperature ranges may be defined (Figure 6): (i) from 0 to 35 °C; $\tau_m \gg T_{1m}$ and the relaxivity is determined by the outer-sphere component which increases as the temperature is reduced; (ii) from 35 to 50 °C; a small and increasing contribution of the inner-sphere relaxivity may be discerned, but the sum of $\tau_m + T_{1m}$ is still dominated by τ_m, which decreases with T, and therefore R_{1p} rises slightly; (iii) above 50 °C; now $\tau_m < T_{1m}$, and the classical behavior of a small anionic chelate is observed with a decrease in R_{1p} as T increases.

Similar considerations apply at lower pH in accounting for the relaxivity behavior, and the NMRD profiles may be fitted well to the data with an appropriate choice of τ_m. For example, the NMRD profile at pH 1 may be accounted for using a τ_m value of 1.1 μs. Such a reduction is rather unlikely to be explained by a change in the proportion of the m isomer (which undergoes faster water exchange), as this ratio was observed to be independent of pH in the range 1−5, in the ^{1}H NMR spectra of the corresponding europium complexes. The NMRD profile may be fitted very well only by changing τ_m; even if 3% metal dissociation had occurred, this would have markedly changed the NMRD profile. That this did not occur, over a period of days, accords with the acid stability defined earlier.

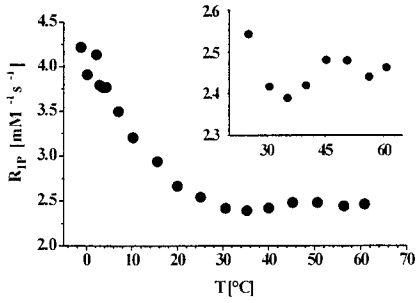

Figure 6. Temperature dependence of the relaxivity of [Gd·**3**]$(CF_3SO_3)_3$ (20 MHz, pH 6).

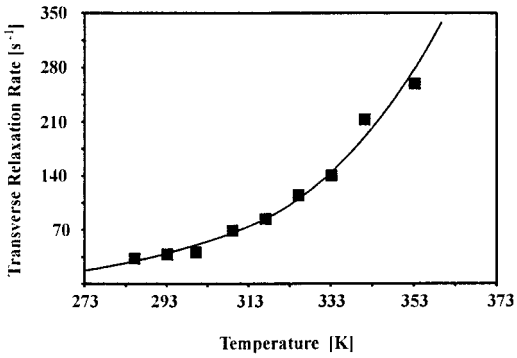

Figure 7. Temperature dependence of the ^{17}O NMR transverse relaxation rate of bulk water in the presence of [Gd·**3**]$(CF_3SO_3)_3$ (49 mM) at 298 K, $\tau_m = 17$ μs.

Proton and Oxygen Exchange. To understand better the pH dependence of the longitudinal proton relaxivity, a variable-temperature, proton-decoupled ^{17}O NMR study was undertaken, probing the nuclear transverse relaxation rate of ^{17}O nuclei in the aqueous solvent. Such a study gives information on the exchange rate of the whole water molecule. At both pH 7 and pH 12 R_{2p} increases with temperature, in the range 0−80 °C (Figure 7), and is consistent with the occurrence of slow to intermediate rates of water exchange[24] (i.e., $R_{2p} \approx 1/\tau_m = k_{ex}$). For [Gd·**3**]$(CF_3SO_3)_3$, the τ_m value was estimated to be 17 μs at 298 K ($\tau_m = 6.9$ μs at 302 K, 30 μs at 288 K, and 215 μs at 277 K). Analogous results were obtained for [Gd·**2**]$^{3+}$ ($\tau_m = 19$ μs, pH 7), and for [Gd·**4**]$^{3+}$ the value was slightly lower ($\tau_m = 7.8$ μs, pH 7). These values are likely to reflect the weighted contribution from the dominant, but slow-exchanging M isomer and the faster exchanging minor m isomer. Indeed solution NMR analysis of a series of [Ln·**2**]$^{3+}$ complexes had earlier suggested that there would be less than 10% of the m isomer present in solution for the analogous Gd complex, above 273 K.

The water exchange rate for [Gd·**2**]$^{3+}$ was also measured to be the same at pH 7 as at pH 12. The fact that the water exchange rate is the same at pH 7 and 12 at first sight seems surprising. A similar lack of variation of the water exchange rate was found for [Gd·**2**]$^{3+}$, with no significant change in the

(23) Hoeft, S.; Roth, K. *Chem. Ber.* **1993**, *126*, 869.
(24) Frey, U.; Merbach, A. E.; Powell, D. H. In *Dynamics of Solutions and Fluid Mixtures by NMR*; Delpuech, J.-J., Ed.; John Wiley & Sons Ltd.: Chichester, 1995; pp 263−307.

rate of water exchange measured at pH 6, 8, and 10. To give insight into the physical basis of this seemingly surprising result, a triangular kinetic reaction scheme may be considered. Similar kinetic schemes[28] are used to account for the behavior of a reactive intermediate in competing substitution reaction mechanisms. In this scheme, it has been assumed that unimolecular dissociation of a hydroxide anion from the (LGdOH) species is very unlikely and that acid catalysis of this step proceeds only via ($LGdOH_2$), i.e., via protonation on the bound hydroxy group.

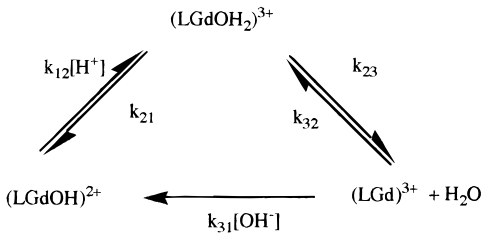

This triangular reaction scheme is characterized by two rate processes,[28] the first of which (eq 3) is associated with the

$$k_1 = k_{12}[H^+] + k_{21} \tag{3}$$

proton-transfer equilibrium, and is expected to be fast. The second process is associated with oxygen exchange and is described by eq 4, in which $K_{12} = 1/K_a$. The pK_a for

$$k_2 = \frac{(k_{23}K_{12})[H^+]}{1 + K_{12}[H^+]} + k_{31}[OH^-] + k_{32} \tag{4}$$

[Gd·**2**(OH_2)]$^{3+}$ has been measured independently by potentiometry to be 7.90[8] (298 K, $I = 0.1$ M NMe_4NO_3), i.e., $K_a = 1.26 \times 10^{-8}$. Equation 4 may be rearranged as follows:

$$k_2 = \frac{k_{23}[H^+]}{[H^+] + K_a} + k_{31}[OH^-] + k_{32} \tag{5}$$

At pH 12, [H^+] tends to zero, so eq 5 simplifies to

$$k_2 = k_{31}[OH^-] + k_{32} \tag{6}$$

Around pH 7, the base and acid concentrations are small, so the term in [OH^-] becomes very small. Given that k_{32} is likely to be greater than k_{23} (i.e., the equilibrium constant for association of water with the (LGd) species is finite, so that the bound water species predominates, in agreement with the K_a value of 33 M^{-1} measured by luminescence methods for [Eu·**3**]$^{3+}$ in MeCN), the equation simplifies to

$$k_2 = k_{32} \tag{7}$$

Thus, the rate of water oxygen exchange may be independent of pH provided that the base concentration is not too high, e.g., in the pH range 6−11. The species $(LGdOH)^{2+}$ must therefore be regarded as inert to oxygen exchange. This analysis confirms that the *fastest* step involved in oxygen exchange is likely to involve the rate of association of water with the short-lived, eight-coordinate gadolinium complex. At the same time, it should be recalled that the *rate-determining* step in dissociative water oxygen exchange is k_{23}, i.e., the loss of water from the nine-coordinate species.

Under the conditions of very slow water exchange found for the cationic tetraamide complexes, the additional contribution to the proton relaxivity observed may be assigned to the occurrence of a prototropic exchange which can be either base or acid catalyzed. In the pH regime 3−7, the prototropic exchange rate is much slower than the water exchange rate, whereas in more acidic or basic media the prototropic exchange rate becomes faster than the water exchange rate, τ_m is then less than T_{1m}, and the relaxivity increases. Hence, the pH dependence of the relaxivity may be fitted by using an expression wherein τ_m is given by the inverse of the sum of the water and prototropic exchange rates.

Prototropic exchange may occur either at the metal-bound water molecule or in the labile amide ligand protons that are close to the paramagnetic center. A potentiometric titration for [Gd·**3**]$(CF_3SO_3)_3$ revealed a pK_a = 7.90(±0.03) (I = 0.1 M NMe_4NO_3, 298 K) associated with deprotonation of the bound water.[8] Therefore, there is a base-catalyzed prototropic exchange process, involving the Gd-bound water, which is common to all three of the amide complexes studied. Deprotonation causes a decrease in the effective "q" value from 1.0 to 0.5, and this is particularly evident in the case of [Gd·**4**]$^{3+}$, where the inner-sphere component makes a detectable contribution to the relaxivity because of the slightly higher value of the water exchange rate. The relaxivity values for [Gd·**3**]$^{3+}$ and [Gd·**2**]$^{3+}$ at pH 11 (Figure 4) are higher than can be accounted for by a reasonable value of the prototropic exchange rate. In these two cases, there must be an additional contribution to the observed relaxivity. Deprotonation of the amide NH protons may occur in very basic media, and for [Gd·**2**]$^{3+}$ a potentiometric titration revealed two pK_a values at 11.02 and 11.89 (I = 0.1 M NMe_4NO_3, 298 K) consistent with stepwise deprotonation of trans-related amide NH protons. Such an exchange process affords an additional mechanism by which the relaxivity may be enhanced,[25] which is not possible for the complex of the dimethylamide derivative [Gd·**4**]$^{3+}$.

Model of the Prototropic Exchange Mechanisms. In accounting for the full pH dependence of the observed relaxivity, three separate pH regimes may be defined. First in the region 4−7, the relaxivity is given as the sum of the inner- and outer-sphere contributions and is determined by the value of τ_m. Water exchange is

$$R_{1p} = R_{1p}^{is} + R_{1p}^{os} \tag{1}$$

where

$$R_{1p}^{is} = \frac{C_{tot}q}{55.6(T_{1m} + \tau_m)} \tag{2}$$

slow and there is no significant prototropic exchange. Thus, for [Gd·**3**]$^{3+}$ using R_{1p}^{os} = 1.8 mM^{-1} s^{-1}, q = 1, and τ_m = 17 μs, an excellent fit of the relaxivity profile is obtained and the values of T_{1m} correspond very well to those obtained by fitting the corresponding NMRD profile. In the pH range 0−3, with a

(25) In accord with this hypothesis, the ^{1}H NMR spectra of [Eu·**2**]$^{3+}$ and [Yb·**2**]$^{3+}$, at pD 7, 11.4, and 12, reveal an increasing proportion of a second solution species, lacking C_4 symmetry.

(26) Bányai, I.; Glaser, J.; Read, M. C.; Sandström, M. *Inorg. Chem.* **1995**, *34*, 2423.

(27) Bruker Analytical X-Ray Instruments (1998) SHELX96: suite of programs for data reduction, solution, and refinement of crystal structures.

(28) Bernasconi, C. F. *Relaxation Kinetics*; Academic Press: New York, 1976; p 51.

Scheme 1. Hypothetical Hydrogen-Bonding Scheme Showing Solvent-Separated Ion Pairs

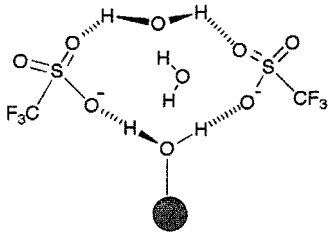

triflate counterion, an acid-catalyzed process may be invoked (eq 8). A good fit to the observed data is obtained when $k_{aex} =$

$$R_{1p}^{is} = \frac{C_{tot}q}{55.6}\left(\frac{1}{T_{1m} + 1/(k_{ex} + k_{aex}[H^+])}\right) \quad (8)$$

2×10^6 s^{-1}. The relaxivity increase in the acidic pH region 0−3 is reversible and may not reasonably be ascribed to dissociation of one or more of the pendant arms (giving a higher "*q*" value) because the luminescence measurement of *q* on the related Eu complex gave the same value of 1.1(±0.2) at pH 1, 2, and 5. Information on the nature of the acid-promoted relaxation enhancement has been gained by measuring the longitudinal relaxation time T_1 of the ^{19}F nuclei in the triflate counterions. In the presence of 40 mM CF_3SO_3Na, a solution containing 2 mM [Gd·**3**](CF_3SO_3) gave rise to a sufficiently intense ^{19}F resonance to allow T_1 measurements to be made. In the pH range 8−2, the T_1 value was constant (∼75 ms) but increased abruptly as the pH fell below 2, indicative of a longer distance between the fluorinated anion and the paramagnetic center. It is possible that long-lived, strong ion pair interactions (Figure 1 and Scheme 1) occur above pH 2 which are progressively weakened as the H_3O^+ concentration increases: the onset of the breakup of these ion pairs is a sensitive function of the nature of the counteranion, and addition of excess Cl^- or SO_4^{2-} caused the ^{19}F T_1 to increase significantly at higher pH values. The separation of the [Gd·**3**]$^{3+}$/$X^{\ominus}$ ion pairs may be related to the establishment of a lower energy pathway for proton exchange from the coordinated water molecule to the bulk. Such a process could involve a proton transfer to the second hydration sphere hydrogen-bonded water molecules, as has been shown to take place for the kinetically inert $[Rh(H_2O)_6]^{3+}$ species.[26] Further aspects of this behavior will be defined in a forthcoming publication.

Finally, in the pH region above 7, allowance must be made for the base-catalyzed exchange of both the bound water protons and the proximate amide NH protons (eqs 9 and 10).

$$\underset{C_A}{MLH_2(OH_2)} \overset{K_a}{\rightleftharpoons} \underset{C_B}{MLH_2OH} + H^+ \quad (9)$$

$$MLH_2(OH) \overset{K_a'}{\rightleftharpoons} ML(OH) + 2H^+ \quad (10)$$

The processes are depicted schematically in Scheme 2. The relaxivity in the basic pH regime may then be given as

$$R_{1p}^{is} = \frac{C_A q}{55.6(T_{1m} + 1/(k_{ex} + k_{bex}[OH^-]))} + \frac{C_B q k}{55.6(T_{1m} + (1/(k_{ex} + k_{bex}[OH^-]))} + \frac{C_C w}{55.6}\frac{1}{T_{1m}''} \quad (11)$$

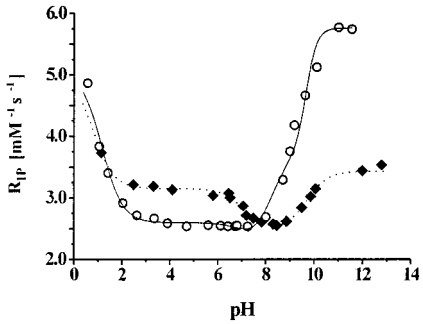

Figure 8. pH dependence of the relaxivity of [Gd·**4**](CF_3SO_3)$_3$ and [Gd·**3**](CF_3SO_3)$_3$ (open circles), (20 MHz, 298 K), showing the fit to the experimental data.

wherein

$$C_B = \frac{K_A C_{tot}}{K_a + [H^+]}$$

$$C_A = C_{tot} - C_B$$

$$C_C = \frac{K_a' C_B}{K_a' + [H^+]^2}$$

and $k = 0.5$, $w = 2 =$ the number of second-sphere water molecules, and $T_{1m}'' = 1.9 \times 10^{5-}$ s = the longitudinal water proton relaxation time for the ligand deprotonated species at high pH. For [Gd·**4**]$^{3+}$, amide deprotonation cannot occur, and the relaxivity profile (Figure 8, Table 2) is fitted well with a pK_a for the bound water of 7.01 and a value for the base-catalyzed proton exchange rate, k_{bex}, of 6×10^9 s^{-1}. Such a value is about 1 order of magnitude higher than that found in pure water and is similar to the rate of prototropic exchange catalyzed by buffer anions.[29] For [Gd·**2**]$^{3+}$ and [Gd·**3**]$^{3+}$, allowance needs to be made at higher pH for successive amide deprotonation. It is reasonable to assume that NH deprotonation promotes the formation of a well-defined second hydration sphere, in which water molecules may hydrogen bond cooperatively to the amide center and the bound hydroxyl group. This hypothesis allows an excellent fitting of the relaxivity data (Figure 8) to be obtained, when two ($w = 2$), rapidly exchanging ($T_{1m''} \gg \tau_{m''}$) "second-sphere" water molecules are considered, and the best fit was obtained for a distance of 3.6 Å between the Gd ion and these second-sphere water molecules.

Conclusion

The cationic gadolinium complexes of 12-N_4-based tetraamide complexes exist in solution as two major isomers, with a square or a twisted square antiprismatic coordination geometry. The relative proportions of these two isomers are governed by the nature of the amide substituents. Water exchange occurs sufficiently slowly at the metal center to limit the observed relaxivity but is about 50 times faster in the twisted antiprismatic complex. This result suggests that new contrast agents may be developed by devising "DOTA-like" complex structures wherein the proportion of this isomer in solution is maximized. Furthermore, the slowness of water exchange in such complexes has allowed the contribution of prototropic exchange to be evaluated for the first time. Base-catalyzed prototropic exchange mechanisms have been identified involving either deprotonation

(29) Hertz, H. G.; Versmold, H.; Yoon, C. *Ber. Bunsen-Ges. Phys. Chem.* **1983**, *87*, 577.

Scheme 2. Base-Catalyzed Prototropic Exchange Mechanisms

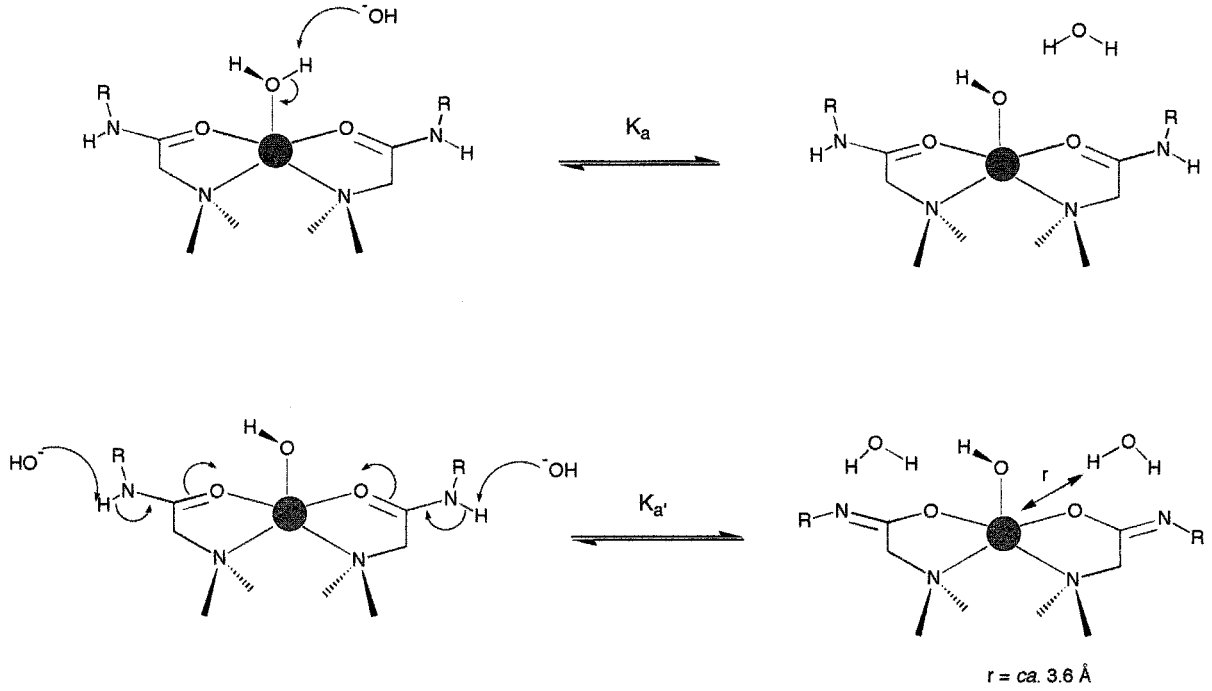

of labile protons on the ligand or deprotonation of the bound water molecule. In more acidic media, the studies reported here are limited to triflate complexes; however, it is likely that higher acid concentrations may cause a breakup of the strongly hydrated tight ion pairs. Indeed the slowness of the water exchange rate at the metal center is likely to be a consequence of the tight ion pairing: the bound water molecule is strongly hydrogen bonded to the counteranion (as seen in the X-ray structural analysis, reported here and elsewhere),[6c] and the unusually high barrier to water exchange may be associated with the need to disrupt not only the primary (water-separated) ion pair but also the well-defined secondary solvation shell associated with such tightly bound ion pairs. Such an interpretation requires that the onset of acid-mediated relaxivity enhancements is anion-dependent, and this effect has been observed in the presence of different anions, and will be discussed in more detail in a subsequent publication.

Experimental Section

General Procedures. Reactions requiring anhydrous conditions were carried out using Schlenk-line techniques under an atmosphere of dry argon. Water was purified by the "Purite$_{STILL}$-plus" TM system. Thin-layer chromatography was carried out on neutral alumina plates (Merck AST 5550) and visualized by iodine staining. Infrared spectra were recorded on a Perkin-Elmer 1600 FT spectrometer using GRAMS-Analyst software; solids were incorporated into KBr disks.

The NMR spectra were acquired using a Brüker AC250 spectrometer operating at 250.13, 62.9, and 235.3 MHz for ^{1}H, ^{13}C{^{1}H}, and ^{19}F-{^{1}H} measurements, respectively, a Varian VXR 200 operating at 200 MHz for ^{1}H, a JEOL EX-90 operating at 90 MHz for ^{1}H and 12 MHz for ^{17}O, a JEOL EX-400 operating at 400 and 100.6 MHz for ^{1}H and ^{13}C{^{1}H}, respectively, and a Varian VXR 400 operating at 400 MHz for ^{1}H. Two-dimensional spectra were run on a JEOL EX-90 and a Varian VXR 200 spectrometer. Variable-temperature ^{1}H NMR studies were carried out on a Varian VXR 400, a JEOL EX-90, and a JEOL EX-400 instrument. Spectra were referenced internally relative to *tert*-butyl alcohol (δ_H 0; δ_C 31.3) for paramagnetic complexes or to the residual protiosolvent resonances, relative to TMS.

Variable-temperature proton-solvent longitudinal relaxation times were measured at 20 MHz at Torino on a Spinmaster spectrometer [Stelar, Mede(PV), Italy] by means of the inversion−recovery technique (16 experiments, 4 scans). The reproducibility in T_1 measurements was within less than 1%. The temperature was controlled by a JEOL airflow heater equipped with a copper−constantan thermocouple: the actual temperature in the probehead was measured with a Fluke 52 k/j digital thermometer with an uncertainty of 0.5 K.

The $1/T_1$ NMRD profiles of water protons were measured over a continuum of magnetic fields from 0.000 24 to 1.2 T corresponding to a 0.01−50 MHz proton Larmor frequency on the Koenig−Brown field-cycling relaxometer installed at the University of Florence, Italy. The temperature inside the probe was controlled by circulation of perfluoroalkanes. Data at higher frequencies were also obtained from JEOL EX-90 and EX-400 spectrometers.

The k_{ex} parameters for {Eu·**2**}$^{3+}$ were obtained by fitting the experimental data obtained on a JEOL instrument at 400 MHz with the DNMR-SIM line-shape simulation program for dynamic NMR spectra (version 1.00, 1994), developed by G. Haegel and R. Fuhler, Institüt fur Anorganische Chemie, Universität Dusseldorf (available on the Internet at http://www.uni-dusseldorf.de/WWW/Mathnat/AC1/forsch.ung/nmr/dnmr-sim.htm). In the fitting procedure the chemical shift difference between the two exchanging peaks was allowed to vary to some extent, to allow for the temperature dependence of the paramagnetic shift (ca. 0.46 ppm/K over the range 230−241K). For [Eu·**3**]$^{3+}$, the rate of water exchange was assessed on Varian VXR 400 instrument by saturation transfer methods, measuring the relaxation rate of the bound water proton resonance, using the inversion−recovery method (e.g., $R_1 = 337(\pm 20)$ s^{-1} at 264.5 K). The integral of the bound water peak was measured in the absence and presence of saturation of the free water signal (at ca. 2.5 ppm). The probe temperature was calibrated using the MeOH chemical shift thermometer (±0.3 K), and the resonance of the most shifted axial ring proton at ca. 33 ppm was used as an internal calibrant for the integration measurements of the bound and free water signals.

Electrospray mass spectra were recorded on a VG Platform II (Fisons) instrument, operating in positive ion mode.

Ligand and Complex Synthesis. The tetraamide ligands **2** and **4** were prepared following published procedures,[6a,11] and crystals of ligand **1** were obtained as the oxonium salt of the dihydrochloride from dilute aqueous HCl (Table 1).

1,4,7,10-Tetrakis[(*N*-methylcarbamoyl)methyl]-1,4,7,10-tetraazacyclododecane (3). To a solution of 1,4,7,10-tetracyclododecane (2.09 g, 11.6 mmol) in dry ethanol (50 mL) were added potassium carbonate

(6.45 g, 46.7 mmol) and *N*-methylchloroethanamide (5.46 h, 50.7 mmol). The mixture was heated under reflux for 48 h, solvent was removed under reduced pressure, and the residue was taken up in hot ethanol, filtered, and cooled. Slow addition of diethyl ether led to formation of 3.06 g (58%) of a colorless solid. Mp: 207−8 °C. ^{1}H NMR (250 MHz, $CDCl_3$): δ 3.07 (s, 8 H, CH_2CO), 2.81, 2.80 (s + s, 6H + 6H, CH_3N), 2.63 (s, 16 H, ring CH_2N). ^{13}C NMR (62.5 MHz, $CDCl_3$): δ 171.2 (CO), 58.8 (NCH_2CO), 52.8 (CH_2N ring), 25.9 (NMe). IR (KBr): 3283 (ν_{NH}), 3077, 2826 (ν_{CH}), 1667 (ν_{CO}), 1552, 1308, 1264, 1233, 1106 (ν_{CO}), 992, 973, 737, 679, 576 cm^{-1}; Anal. Calcd for $C_{20}H_{42}N_8O_4 \cdot 1.5\ H_2O$: C, 49.6; H, 8.89; N, 23.1. Found: C, 49.4; H, 9.04; N, 23.0. LRESMS: $(M + Na)^+$ 479.7. Crystals of the ligand suitable for X-ray analysis were obtained by slow evaporation of an aqueous solution (Table 1).

Representative Procedure for Lanthanide Complex Formation. [Eu·3](CF$_3$SO$_3$)$_3$·4H$_2$O. To a solution of europium trifluoromethanesulfonate (0.34 g, 0.57 mmol) in dry acetonitrile (15 mL) was added a solution of ligand **3** (0.275 g, 0.60 mmol) in dry methanol (1 mL), and the mixture was heated under reflux for 8 h. The volume was reduced by one-third, and to the cooled solution was added dry tetrahydrofuran until the complex precipitated. The resultant solid was filtered and redissolved in acetonitrile (5 mL) and precipitated again following THF addition. The dried solid, 0.41 g (72%), was isolated as a white powder. Anal. Calcd for $C_{23}H_{40}EuF_9N_8O_{13}S_3 \cdot 4H_2O$: C, 24.5; H, 4.29; N, 9.93. Found: C, 24.3; H, 3.94; N, 9.75. LRESMS: $(M + (CF_3SO_3)_2)^+$ 907.3, $(M)^{2+}$ 379.41, $(M)^{3+}$ 202.94. ^{1}H NMR (300 MHz, CD_3CN, 233 K): δ 86.1 (br s, 2H, bound water), 38.6 (s, 4H, ring CH_2, axial), −0.4 (s, 12 H, NCH_3), −1.8 (s, 4H, ring CH_2 equatorial), −5.4 (s, 4H, NH), −8.1 (s, 4H, ring CH_2 axial), −9.3 (s, 4H, ring CH_2 equatorial), −18.0 (s, 4H, CH_2CO), −19.8 (s, 4H, CH_2CO). At 233 K, the shift for the coordinated water in the minor isomer was +22.2 ppm. IR (KBr): 3676 (ν_{OH}), 3587, 3460 (ν_{NH}), 1607 (ν_{CO}), 1260 (ν_{SO}), 1173, 1045, 1037, 706 cm^{-1}.

[Gd·3](CF$_3$SO$_3$)·4H$_2$O. This complex was prepared in an analogous manner. Anal. Calcd for $C_{23}H_{40}GdF_9N_8O_{13}S_3 \cdot 4H_2O$: C, 24.4; H, 4.27; N, 9.89. Found: C, 24.1; H, 3.78; N, 9.69. LRESMS: $(M + (CF_3SO_3)_2)^+$ 912.0. Gadolinium complexes of **2** and **4** were prepared similarly and give satisfactory microanalytical and LRESMS data.

[Dy·3](PF$_6$)$_3$·3.5H$_2$O. This was prepared as described above and was crystallized from 5% aqueous ammonium hexafluorophosphate solution. Anal. Calcd for $C_{20}H_{40}DyF_8N_8O_4P_3 \cdot 3.5H_2O$: C, 21.5; H, 4.22; N, 10.0. Found: C, 21.3; H, 3.95; N, 9.80. IR (KBr): 3444 (ν_{OH}), 3243 (ν_{NH}), 3109, 1638 (ν_{CO}), 1411, 1165, 839 (ν_{PF}) cm^{-1}. ^{1}H NMR (90 MHz, 293 K, pD 6): δ 241 (br s, 4H, CH_2CO), 126 (br s, 4H, ring CH_2 axial), 79 (br s, 4H, CH_2CO), 39 (12H, CH_3N), −92 (br s, 4H, ring CH_2 equatorial), −94 (br s, 4H, ring CH_2 equatorial), −390 (4H, br s, ring CH_2, axial).

[Eu·2](CF$_3$SO$_3$)$_3$·4H$_2$O. Anal. Calcd for $C_{19}H_{32}EuF_9N_8O_{13}S_3 \cdot 4H_2O$: C, 21.3; H, 3.74; N, 10.4. Found C, 21.0; H, 3.50; N, 10.1. ^{1}H NMR (400 MHz, CD_3CN (400 μL + 5 μL of H_2O), 232 K): δ (major isomer) 84.1 (br s, 2H, bound H_2O), 38.2 (s, 4H, ring CH_2, axial), 0.61 (s, 4H, ring CH_2 equatorial), −1.51 (s, 4H, CONH), −5.31 (s, 4H, CONH′), −8.78 (s, 4H, ring CH_2 axial), −9.31 (s, 4H, ring CH_2 equatorial), −18.0 (s, 4H, CH_2CO), −18.4 (s, 4H, CH_2CO); (minor isomer) 19.0 (br s, 2H, bound water), 7.41 (s, 4H, ring CH_2 equatorial), 7.40 (s, 4H, ring CH_2 axial), 3.57 (s, 4H, CONH), 2.43 (s, 4H, CH_2-CO), −1.52 (s, 4H, ring CH_2, axial), −3.64 (s, 4H, CH_2CO), −10.4 (s, 4H, CONH′), −13.1 (s, 4H, ring CH_2 equatorial).

[Eu·4](CF$_3$SO$_3$)·3H$_2$O. Anal. Calcd for $C_{27}H_{48}EuF_9N_8O_{13}S_3 \cdot 3H_2O$: C, 27.8; H, 4.63; N, 9.60. Found: C, 27.5; H, 4.31; N, 9.40. LRESMS: $(M + (CF_3SO_3)_2)^+$ 960.7, $(M)^{2+}$ 406.3, 407.4, $(M)^{3+}$ 221.4, 222.0. ^{1}H NMR (400 MHz, pD 6, 273 K): δ (major isomer/twisted antiprismatic structure) 9.7 (s, 4H, ring CH_2 axial), 1.70 (s, 12H, NCH_3), 0.8 (s, 12H, NCH_3), −1.20 (s, 4H, CH_2CO), −2.3 (s, 4H, ring CH_2, axial), −6.2 (s, 4H, CH_2CO) −9.6 (s, 4H, ring CH_2 equatorial), −11.9 (s, 4H, ring CH_2 equatorial) (minor isomer/square antiprism) 35.8 (s, 4H, ring CH_2 axial), 2.3 (s, 12H, NCH_3), −1.4 (s, 4H, ring CH_2 equatorial), −0.9 (s, 12H, NCH_3), −8.3 (s, 4H, ring CH_2 equatorial), −10.4 (s, 4H, ring CH_2 axial), −17.5 (s, 4H, CH_2CO), −17.9 (s, 4H, CH_2CO).

Crystallography. Single-crystal X-ray diffraction experiments were carried out at 150 K for the ligands using a Rigaku AFC6S four-circle diffractometer (ω-scan mode for **1** and $\omega-2\theta$ for **3**). Graphite-monochromated Cu Kα radiation (λ = 1.541 84 Å) and an Oxford Cryostream open-flow N_2 gas cryostat were used. The experiment with [Dy·**3**(H_2O)](PF_6)$_3$ was carried out on a Siemens SMART-CCD diffractometer using graphite-monochromated Mo Kα radiation (λ = 0.710 73 Å). The structures of the ligands were solved by direct methods, and the complex was solved by Patterson and Fourier methods and refined by full-matrix least squares against F^2 for all data using SHELXTL software.[27] All non-H atoms, excluding solvent, were refined with anisotropic displacement parameters; all H atoms were located from difference Fourier maps (or were placed in calculated positions where necessary) and were refined in isotropic approximation. Data are summarized in Table 1, and atomic coordinates and displacement parameters and bond distances and angles have been deposited at the Cambridge Crystallographic Data Centre.

Acknowledgment. We thank the EU-COST program, Bracco S.p.A. (S.A., M.B.), the Medical Research Council (A.A.d.S.), the EPSRC (M.W., J.I.B.), the Royal Society (Leverhulme Trust Senior Research Fellowship, D.P.), the EU-BIOMED program for a fellowship (A.B.), Dr. M. Crampton (University of Durham) for stimulating discussions concerning kinetic analysis, and the reviewers for constructive critical comment.

Supporting Information Available: A summary table of crystallographic information and figures of the X-ray structure of **3**, of diprotonated DOTA, $H_3O^+[H \cdot Cl_2]$, a representative example of the rate of dissociation of the complex, and ln k vs T^{-1} plots for [Eu·**3**]$^{3+}$ (PDF). This material is available free of charge via the Internet at http://pubs.acs.org.

JA990225D